New Journal of Physics
The open-access journal for physics

Nonlinear structures of strongly coupled complex plasmas in the proximity of a presheath/sheath edge

V V Yaroshenko[1,4], V Nosenko[1], M A Hellberg[2], F Verheest[2,3], H M Thomas[1] and G E Morfill[1]

[1] Max-Planck-Institut für extraterrestrische Physik, Giessenbachstrasse, Postfach 1312, 85741 Garching, Germany
[2] School of Physics, University of KwaZulu-Natal, Private Bag X54001, Durban 4000, South Africa
[3] Sterrenkundig Observatorium, Universiteit Gent, Krijgslaan 281, B-9000 Gent, Belgium
E-mail: viy@mpe.mpg.de

New Journal of Physics **12** (2010) 073038 (12pp)
Received 26 April 2010
Published 27 July 2010
Online at http://www.njp.org/
doi:10.1088/1367-2630/12/7/073038

Abstract. The formation of a steady-state nonlinear potential structure of a double-layer type near the presheath/sheath edge of a plasma discharge is theoretically investigated in complex plasmas containing Boltzmann electrons, cold fluid ions and strongly coupled microparticles. Equilibrium of the particles is provided by the electrostatic force and an effective 'dust pressure' associated with electrostatic interactions between the highly charged grains. The results are of importance for complex plasma experiments in microgravity conditions, for thermophoretically levitated configurations and for processing plasmas loaded by nanometer-sized microparticles.

Contents

[4] Author to whom any correspondence should be addressed.

1. Introduction

While all complex plasma experiments reveal well-defined boundaries between different plasmas, we only know of a few attempts to treat this problem. Different aspects of the physical processes at the plasma interfaces have been investigated theoretically [1]–[9] and experimentally [10, 11]. One of these studies predicts an electrostatic double layer (DL) arising at the boundary between the complex plasma and the electron–ion plasma [6]. This treatment, however, was not self-consistent, as the issue of the dust equilibrium state was sidestepped. Several papers then followed to include the particle steady state and formulate conditions favoring the formation of an electrostatic double layer at the plasma interface in the case of a dense dust cloud due to ionization of neutral atoms by 'hot' electrons [12, 13].

In this paper, we continue the study of plasma discharges in the presence of highly charged microparticles and find the equilibrium electrostatic potential as an exact solution of the Poisson equation in the vicinity of the transition from quasineutral to charged plasmas. Such a solution self-consistently determines the plasma densities. We focus on the case where the gravitational force on the microparticles is negligibly small, and one can introduce a dust steady state associated with electrostatic interactions between the strongly coupled particles [14]. Such an approach reduces the nonlinear problem to a Sagdeev pseudopotential formalism. Nonlinear structures of the double-layer type are then studied in terms of the existence domain in a physically meaningful parameter space. In particular, we show that, under certain conditions, the presence of the highly charged microparticles can lead to a remarkable effect on the plasma potential near the sheath edge: an electrostatic double layer appears and confines the particles, and thus provides in a natural way the sharp plasma boundaries, even at low dust number density.

2. Nonlinear formalism

To study the influence of charged microparticles on the electric potential profile near the sheath edge, we consider a one-dimensional (1D) model of the collisionless discharge [14], assuming that there is no appreciable electric field in the bulk plasma, where the charge quasineutrality holds,

$$n_{e0} + Z_d n_{d0} - n_{i0} = 0. \tag{1}$$

Here, n_{e0}, n_{i0} and n_{d0} denote the electron, ion and dust number density in the bulk plasma, respectively, and Z_d refers to the particle charge number. We assume that the transition from a quasineutral plasma to the charged layer of the sheath mainly occurs near the presheath/sheath edge, which we put by definition at $x = 0$. The electric potential φ is then zero far away from the sheath ($x \to -\infty$), while, in the immediate vicinity of the sheath edge and inside the charged layer, φ is determined by Poisson's equation,

$$\frac{d^2\varphi}{dx^2} = 4\pi e\,(n_e + Z_d n_d - n_i)\,, \tag{2}$$

with the respective plasma number densities n_e, n_i and n_d.

The electron density can be described by the usual Boltzmann distribution,

$$n_e = n_{e0}\,\exp(e\varphi/T_e), \tag{3}$$

with kinetic temperature T_e. The positive ions are accelerated by the sheath electric field to velocities higher than the ion thermal velocity, and their number density can be determined from the steady-state momentum and continuity equations as [14]

$$n_i = \frac{n_{i0}}{\sqrt{1 - 2e\varphi/\left(m_i V_{i0}^2\right)}}, \tag{4}$$

where V_{i0} denotes the ion velocity outside the sheath ($x \to -\infty$) and m_i refers to the ion mass.

The equilibrium state of the heavy plasma component—the charged particles—results from the balance of all the forces acting on the microparticles, including the electrostatic, plasma drag, gravitational and pressure gradient forces. In this paper, however, we address the situation when the gravitational force acting on the particles is negligible, the particles are strongly coupled and the dust cloud extends over the discharge plasma occupying the volume up to a boundary presheath/sheath. These conditions could be relevant for studies of complex plasmas under microgravity conditions (see, e.g., [15]–[18]), for thermophoretically levitated systems [19], for experiments on nanoparticle coagulation [20] and for processing plasmas dealing also with very small (submicron/nanometer-sized) particles [21, 22].

On the periphery of the discharge, the microparticles usually do not show a directed motion but vibrate near their equilibria. The particle steady state is mainly provided by two forces: the electrostatic force, $F = eZ_d d\varphi/dx$, and the force due to the gradient of the internal 'electrostatic pressure', $n_d^{-1} dP_d/dx$, originating from the repulsion of similarly charged microparticles [12, 14, 23]. For Yukawa-type interacting strongly coupled grains, P_d can be expressed in terms of an effective dust 'temperature' [14],

$$P_d \simeq T_d^{(\mathrm{eff})} n_d, \tag{5}$$

with $T_d^{(\mathrm{eff})}$ given by

$$T_d^{(\mathrm{eff})} = \frac{N_{nn}}{3} \Gamma T_d (1+\kappa) e^{-\kappa}. \tag{6}$$

Here, T_d denotes the particle kinetic temperature and N_{nn} is the number of nearest neighbors in the crystalline structure ($N_{nn} = 12$ for the fcc and hcp lattices and $N_{nn} = 8$ for the bcc lattice). Finally, Γ is the coupling parameter,

$$\Gamma = \frac{Z_d^2 e^2}{T_d \Delta},$$

with Δ and κ being the mean interparticle distances (the latter is normalized to the plasma screening length λ_D: $\kappa = \Delta/\lambda_D$).

The quantity $T_d^{(\mathrm{eff})}$ is in general a function of the plasma parameters. To specify this dependence, we insert the crystal–liquid approximation $\Gamma = 106 \exp(\kappa)/(1+\kappa+\kappa^2/2)$ [24] in the definition of the effective temperature (6), which yields

$$T_d^{(\mathrm{eff})} \propto \frac{1+\kappa}{1+\kappa+\kappa^2/2}. \tag{7}$$

This immediately confirms a weak functional dependence of $T_d^{(\mathrm{eff})}$ on κ. Moreover, κ, in turn, is characterized by a weak dependence on microparticle density, since $\kappa \propto (n_d)^{-1/3}$. Both these factors imply a weak dependence $T_d^{(\mathrm{eff})}$ on the dust density and eventually lead

to $T_{\rm d}^{(\rm eff)}(\mathrm{d}n_{\rm d}/\mathrm{d}x) \gg n_{\rm d}(\mathrm{d}T_{\rm d}^{(\rm eff)}/\mathrm{d}x)$. The latter means that the characteristic scales of $T_{\rm d}^{(\rm eff)}$ variations are much larger than those of $n_{\rm d}$. Therefore, in a first approximation, we can neglect the weak dependence of $T_{\rm d}^{(\rm eff)}$ on the dust density variations and assume $T_{\rm d}^{(\rm eff)} \simeq T_{\rm d}^{(\rm eff)}(\kappa_0)$, where $\kappa_0 \simeq n_{\rm d0}^{-1/3}$ corresponds to interparticle separation in the quasineutral plasma.

As a result of a balance between electrostatic and effective 'pressure' forces on the charged microparticles, a Boltzmann-like distribution is then recovered [14],

$$n_{\rm d} = n_{\rm d0}\ \exp(eZ_{\rm d}\varphi/T_{\rm d}^{(\rm eff)}) = n_{\rm d0}\ \exp(-Z_{\rm d}\phi/\gamma), \tag{8}$$

with the dimensionless potential given by $\phi = -e\varphi/T_{\rm e}$ and $\gamma = T_{\rm d}^{(\rm eff)}/T_{\rm e}$. As explained elsewhere [12], the exponent of the dust distribution $Z_{\rm d}/\gamma$ is related to the equilibrium dust density $n_{\rm d0}$. Indeed, in the crystal–liquid approximation [24], one finds

$$\frac{Z_{\rm d}}{\gamma} = \frac{3\left(1+\kappa+\kappa^2/2\right)\kappa^3}{N_{nn}\times 106(1+\kappa)}\tau n_{\rm i0}\lambda_{\rm D}^3 p = \beta p, \tag{9}$$

where $\tau = T_{\rm e}/T_{\rm i}$ is the electron–ion temperature ratio and $p = Z_{\rm d}n_{\rm d0}/n_{\rm i0}$ determines the Havnes parameter in the bulk plasma. The parameter β introduced here is a measure of the effective dust 'temperature' with respect to $T_{\rm e}$ at fixed plasma densities, viz $\beta = (T_{\rm e}/T_{\rm d}^{(\rm eff)})(n_{\rm i0}/n_{\rm d0})$. In complex plasma experiments, the characteristic values lie typically in the ranges $\tau \simeq 80-150$; $n_{\rm i0}\lambda_{\rm D}^3 \simeq 10^3 - 10^4$; and $\kappa \simeq 1-2$, so that (9) gives the coefficient β typically between 10^2 and 10^3. This immediately means that, for Havnes parameters $p \gtrsim 0.1$, due to the large exponent $Z_{\rm d}/\gamma = \beta p$ in (8), even small variations in the plasma potential would provide a considerable effect on the dust distribution.

Inserting the plasma densities (3), (4) and (8) in Poisson's equation (2) for the plasma potential within the presheath/sheath region, and integrating this in the traditional way, one obtains

$$\frac{1}{2}\left(\frac{\mathrm{d}\phi}{\mathrm{d}X}\right)^2 + V(\phi, M) = 0, \tag{10}$$

with an analogue of the Sagdeev potential $V(\phi, M)$ given by

$$V(\phi, M) = \frac{M^2}{1-p}\left(1-\sqrt{\frac{2\phi}{M^2}+1}\right) + \left(1-\mathrm{e}^{-\phi}\right) + \frac{1}{(1-p)\beta}\left(1-\exp\left(-\beta p\phi\right)\right). \tag{11}$$

In equations (10) and (11), we have used a dimensionless coordinate $X = x/\lambda_{\rm De} = x/\sqrt{T_{\rm e}/(4\pi e^2 n_{\rm e0})}$, and the Mach number $M = V_{\rm i0}/\sqrt{T_{\rm e}/m_{\rm i}} = V_{\rm i0}/V_{\rm s}$ characteristic for pristine electron–ion plasmas.

Expression (11) looks like the pseudopotential for ion acoustic solitary waves in a plasma with cold ions and a double Boltzmann electron distribution, for which, for appropriate plasma parameter values, 'rarefactive' (negative potential) double layers may be found [25]. One would thus expect such structures to be supported in this case, too. However, there is an important difference from the standard two-electron case: in that case, the argument of the exponential in the last term involves a normalized temperature of the cool electrons, which is an independent parameter. Here, in equation (11), the factor $Z_{\rm d}/\gamma = \beta p$ depends on the Havnes parameter, p. Thus, the p-dependence of our results is expected to differ from what is obtained for the two-electron model [25].

Finally we stress that, unlike the standard Sagdeev approach, which is based on an analysis in the frame of a solitary wave of constant shape and speed, our study relates to a nonlinear structure that is stationary in the laboratory frame. However, as shown in equation (4), the ions drift through the structure (in this case, as indicated above, due to the sheath electric field), much as stationary ions drift through the structure in the wave frame of the moving double layer [25]. The Sagdeev formalism based on equation (11) can thus be pursued and will be applied to possible stationary structures below.

3. Double-layer structures

The discussion of possible solutions of (10) is now reminiscent of what happens in classical mechanics with a classical particle of unit mass moving with velocity $\mathrm{d}\phi/\mathrm{d}X$ in a potential well $V(\phi, M)$ (where M appears as a parameter). From the generic behavior of the Sagdeev pseudopotential, we know that the presence of a second 'Boltzmann' species in (11) can lead to different nonlinear solutions of (10) [25, 26]. We, however, are interested in physically meaningful solutions that obey our initial assumptions of vanishing ϕ at $x \to -\infty$ and finite $\phi \neq 0$ at $x \gtrsim 0$. Also, keeping in mind the results of previous studies of the plasma potential in complex plasma discharges [12, 13], nonlinear solutions of the DL type can satisfy both the aforementioned requirements and should be examined as most appropriate.

For the existence of DL structures, one needs two successive double roots of the pseudopotential $V(\phi, M)$, so that, in the parlance of classical mechanics, ϕ can transit from one value to another without coming back, with a rather sharp and shock-like or kink-like transition between the two. The Sagdeev potential should therefore satisfy

$$V_{\phi=0} = 0, \quad \left(\frac{\mathrm{d}V}{\mathrm{d}\phi}\right)_{\phi=0} = 0, \tag{12}$$

$$V_{\phi=\phi_\mathrm{m}} = 0, \quad \left(\frac{\mathrm{d}V}{\mathrm{d}\phi}\right)_{\phi=\phi_\mathrm{m}} = 0. \tag{13}$$

In addition, there is the requirement that the roots $\phi = 0$ and $\phi = \phi_\mathrm{m}$ correspond to local maxima of $V(\phi, M)$. Note that the requirement $(\mathrm{d}^2V/\mathrm{d}\phi^2)_{\phi=0} < 0$ leads to the Bohm sheath condition on the ion velocity. In our case, the value of the ion velocity can be crucially reduced due to the presence of strongly coupled microparticles and the Mach number satisfies [14]

$$M \gtrsim M_\mathrm{s} = \sqrt{\frac{1}{1 - p + \beta p^2}}. \tag{14}$$

The Bohm speed M_s is the true acoustic speed in this system and is the minimum speed for the support of solitons or double layers. The value of M in (14), however, cannot be smaller than $M_\mathrm{min} = \tau^{-1/2} \sim 0.1$ for applicability of the cold ion approximation (4).

The DL conditions (12)–(14) impose rather stringent restrictions on the values of complex plasma parameters, which might be appropriate in the relevant parameter space.

We will start with a weakly nonlinear approach, based on the assumption $\phi \ll 1$ and an expansion of the Sagdeev potential (11) in powers of ϕ, i.e.

$$\frac{1}{2}\left(\frac{\mathrm{d}\phi}{\mathrm{d}X}\right)^2 + A\phi^2 + B\phi^3 + C\phi^4 + D\phi^5 + \cdots = 0. \tag{15}$$

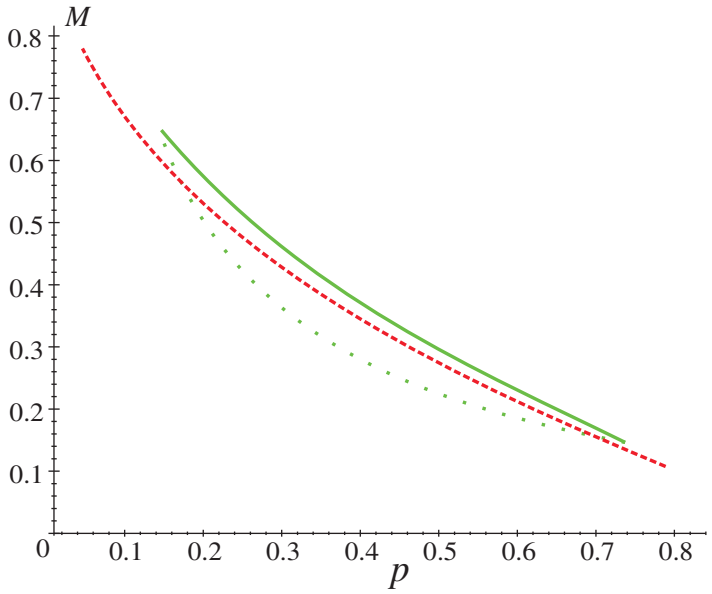

Figure 1. Domain in the $\{p, M\}$-parameter space for the appearance of stable DL structures at the sheath boundary for different β: $\beta = 10^2$ (solid curve) and $\beta = 10^3$ (dashed curve). For given p, admissible M are found between the upper and the lower curves. The dotted line represents the acoustic (Bohm) speed (14), and hence leads to the cut-offs at high and low p.

The expansion up to ϕ^4 can give an analytical DL solution of the type

$$\phi = -\frac{B}{2C}\left\{1 + \tanh\sqrt{\frac{|A|}{2}}X\right\}, \tag{16}$$

which satisfies the initial condition ($\phi \to 0$ when $x \to -\infty$). However, the existence of the solution (16) implies a few conditions to be fulfilled. One is that $A < 0$ (a modified Bohm sheath criterion (14)), and the other requires that the polynomial $A\phi^2 + B\phi^3 + C\phi^4 = C\phi^2(\phi - \sqrt{A/C})^2$ has a double root, i.e. a compatibility condition $B^2 = 4AC$ must be fulfilled. Finally for consistency, the terms that were left out of the expansion (15) have to be small enough or, in other words, $|BD/2C^2| \ll 1$ must hold. As we have checked numerically, in complex plasmas with Boltzmann-distributed dust (8) and realistic values of the coefficient $\beta \sim 10^2$–10^3, one can only obtain weak DL solutions (16) if the last condition $|BD/2C^2| \ll 1$ is ignored. However, no such solutions can be found when the calculations are carried out properly.

To examine the possibility of having DLs that are not weak, we analyze the full Sagdeev potential (11). Figure 1 represents the range of the DL existence in the parameter space $\{p, M\}$ for the given exponent β in the dust distribution. The lower curve expresses the DL conditions for the maximal coefficient $\beta = 10^3$ and the upper one for a minimal value of $\beta = 10^2$. The two curves of admissible $M(p)$ are limited at low and high values of the Havnes parameter. These cut-offs result from the modified Bohm condition (14), as shown in figure 1 for $\beta = 10^2$ (dotted curve). With an increase in β, the range of acceptable p according to (14) grows and, for $\beta \simeq 10^3$, the curve can be continued to the right up to $p \sim 1$, but this part has been omitted because already at $p \sim 0.8$ a value of M is close to the lower limit $M_{\min} = \tau^{-1/2} \simeq 0.1$. There appears to be a strong dependence on p of the value of M at which the DL occurs ($M_{\rm dl}$).

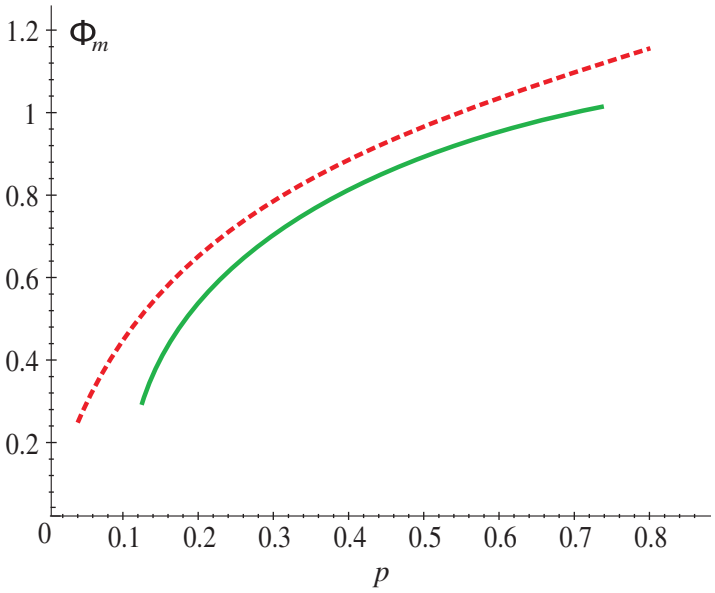

Figure 2. DL amplitude versus p for $\beta = 10^2$ (solid curve) and $\beta = 10^3$ (dashed curve).

However, in part that reflects the fact that the lower Mach number limit, M_s, depends on p (see equation (14)).

Both plots in figure 1 demonstrate a similar decrease in admissible Mach numbers with a growth of microparticle charge density (the Havnes parameter p), showing almost a linear dependence $M \propto (1 - p)$. On the other hand, for reasonable β, the plots do not reveal a significant difference in the DL conditions. Taking, for example, $\beta = 10^3$ and $p = 0.21$ results in $M = 0.516$. For the lower value of $\beta = 10^2$, the DL at the same $p = 0.21$ occurs at a slightly higher velocity $M = 0.54$. It is noteworthy that the DL existence range is weakly dependent on the specific value of the coefficient β. One can therefore expect that, for quite different strongly coupled plasmas, the value of the Havnes parameter p ultimately prescribes, through the admissible M, a spatial position of the DL structure.

Figure 2 illustrates the DL amplitude corresponding to the two limiting values of $Z_{\rm d}/\gamma$. It is seen that in both cases, the DL amplitude grows with the dust density (p). However, the effect of the different coefficients β for the DL amplitude in figure 2 becomes more pronounced than that for the admissible M shown in figure 1.

The typical shape of the Sagdeev potential allowing for the DL structures is shown in figure 3. Calculations have been made at $p = 0.14$, but using two different sets of other parameters, namely $\beta = 250$, $M = 0.61$ and $\beta = 750$, $M = 0.596$. These provide the existence of DL structures with amplitudes $\phi_{\rm m} \simeq 0.51$ and $\phi_{\rm m} \simeq 0.55$, respectively.

As an illustration of the steady-state DL-like structure arising at the sheath boundary, we present a numerical solution of (10) in figure 4, calculated for $p = 0.14$, $M = 0.61$ and the parameter $\beta = 250$. The solid line corresponds to the exact solution of (10), thus representing the potential ϕ as a function of X. One immediately finds the typical shock-like behavior for the plasma potential. Such potential variations result in an abrupt reduction in the dust density, $n_{\rm d}/n_{\rm d0}$, developing on length scales of a few electron Debye lengths, typical of an electrostatic sheath. The potential jump thus separates the complex plasma and the presheath/sheath region,

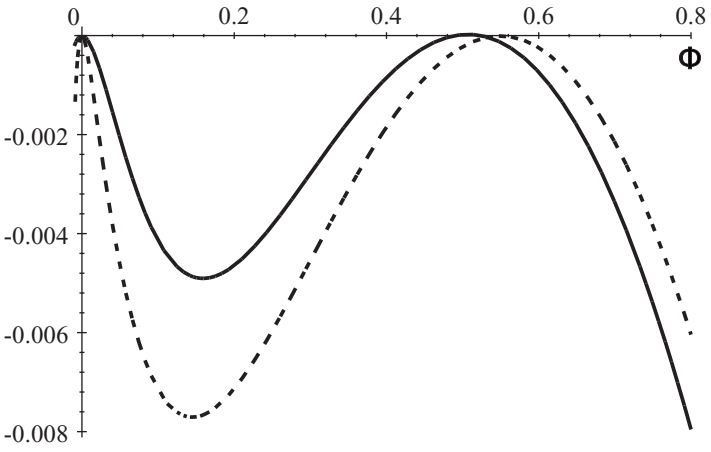

Figure 3. Sagdeev potential for the occurrence of DL solutions. Calculations are made at the same Havnes parameter $p = 0.14$, but for two different exponents: $\beta = 250$, which requires $M = 0.61$ (solid curve); and $\beta = 750$, for corresponding $M = 0.596$ (dashed curve).

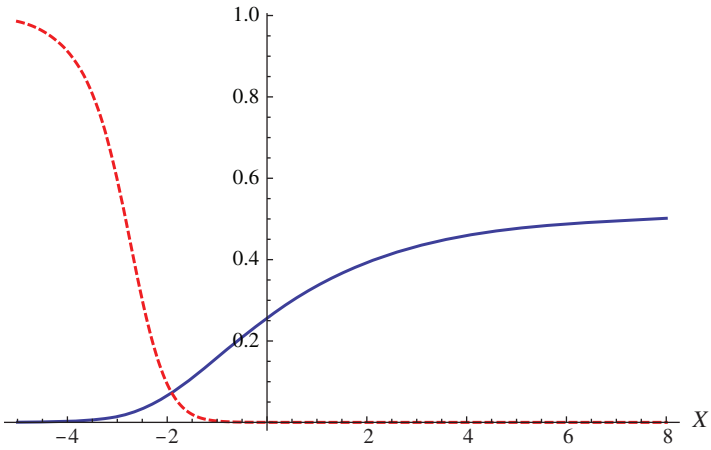

Figure 4. DL-like solution of equation (10) for the normalized plasma potential ϕ (solid curve) and the normalized dust density, n_d/n_{d0} (dashed curve), in the vicinity of the sheath edge. Calculations have been made for $p = 0.14$, $M = 0.61$ and $Z_d/\gamma = 250p = 35$.

as illustrated in figure 4 by the dashed curve. Moreover, it also provides local variations in the dust density near the sheath boundary: the localized increase in interparticle distances developing in the direct vicinity of the plasma boundary (figure 5).

To compare our results to experimental observations, one needs to measure the variations in interparticle distances developing on length scales of a few Debye lengths in the vicinity of a plasma interface. For 3D configurations, reliable measurements are difficult to obtain due to the lack of proper 3D imaging techniques. A careful inspection of different dust particle configurations reveals that for monolayer (2D) plasma crystals the expected effect is well pronounced and can be reliably measured. Indeed, the monolayer experiments clearly

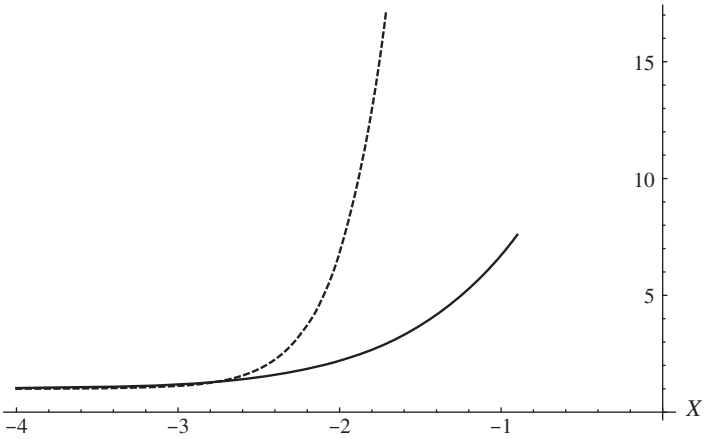

Figure 5. Variation of the normalized interparticle separation, $(n_d/n_{d0})^{-1/3}$, in the proximity of the sheath boundary calculated for the parameters of figure 3.

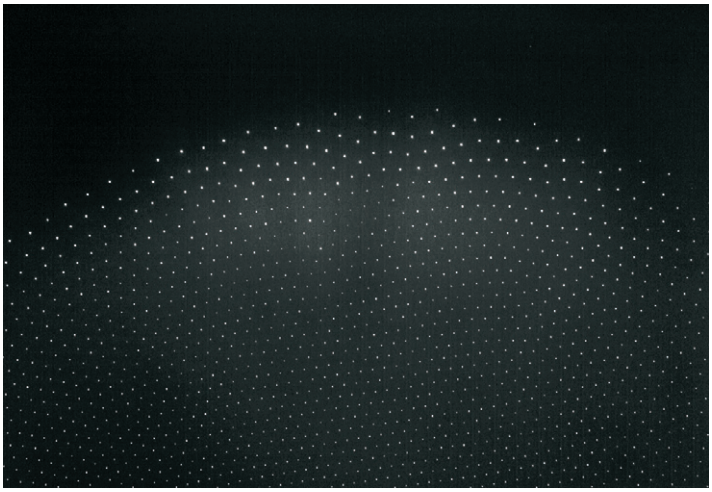

Figure 6. Sharp edge of a 2D plasma crystal. A monolayer of plastic microspheres was suspended in the plasma sheath above the lower electrode in a capacitively coupled rf discharge in argon at 0.66 Pa. Monodisperse particles with a diameter of $9.19 \pm 0.14\,\mu$m were used; particles near the crystal edge appear brighter because the illuminating laser sheet matches perfectly their vertical position. The field of view is $4.27 \times 2.92\,\text{cm}^2$.

demonstrate that the interparticle distances near the crystal edge are always significantly larger than in the central part of the structure [27, 28]. Although the 2D crystals normally levitate in the sheath of the lower electrode in radio frequency (rf) discharges, where the vertical component of the electric field is large enough to balance gravity, one can think of the application of our theoretical findings to the observed variations of particle surface density (or interparticle distances) developing along the horizontal coordinate.

A typical example of a 2D crystal is shown in figure 6. The experiment was done in an rf discharge in argon at a pressure of 0.66 Pa, with particles of 9.19 μm diameter (the experimental

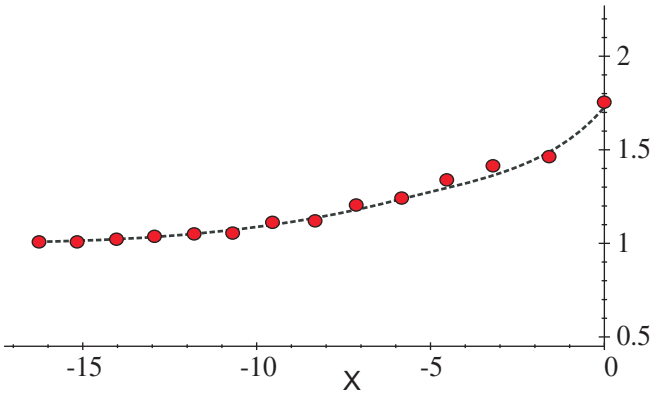

Figure 7. Spatial distribution of the normalized interparticle distance (Δ/Δ_0 with Δ_0 being the average particle separation far away from the crystal boundary) in the proximity of the crystal edge shown in figure 6; $X = 0$ corresponds to the crystal boundary.

setup and plasma parameters are the same as described in [27], but without employment of the additional electrode box). Figure 7 illustrates the variation in normalized particle separations measured in the close vicinity of the boundary ($X = 0$) of this monolayer crystal. Comparing this to the theoretical profiles of figure 5, one can speculate that the horizontal confinement of the monolayer might result from the formation of a potential drop similar to that shown in figure 4. Note that the crystal edge was located far away from the chamber wall in this experiment and therefore we have to exclude the role of the sheath produced by the wall in the initiation of such a potential drop. The potential structure of the DL type along the horizontal direction might form as a result of the existence of a significant ambipolar electric field in the discharge periphery.

4. Conclusions

A theoretical description has been given of the steady-state nonlinear structures of DL type arising near a point where the plasma quasineutrality breaks down (e.g. the presheath/sheath boundary of complex plasma discharges), based on a Sagdeev pseudopotential treatment that was adapted to include the strongly coupled microparticles in microgravity conditions. It has been assumed that the equilibrium of the highly charged particles is provided by the electrostatic force and an effective 'dust pressure' associated with electrostatic interactions between the grains. The nonlinear structures have been characterized in terms of existence domains in a physically meaningful parameter space (figures 1 and 2). First it has been found that weak DL solutions ($\varphi \ll T_e/e$) do not arise near the sheath edge within the model considered. On the other hand, nonlinear solutions with amplitudes up to $\varphi \sim T_e/e$ can easily be self-organized near the plasma/sheath edge. The potential jump results in an abrupt decrease in the dust density, thus providing the plasma separation and sharp plasma interfaces. Interestingly, the range of the DL existence demonstrates a very weak dependence on the specific value of the coefficient β in the dust distribution (see figure 1), where β measures the effective dust 'temperature' ratio at fixed plasma densities. This means that, for strongly coupled plasmas with different β, the value of the Havnes parameter ultimately prescribes through the admissible M the spatial position of

the potential jump and therefore the complex plasma boundary. At the same time, both values p and β determine the slope of the potential profile and the rate of the dust density decrease (figure 5). Increases in one of these result in higher potential jumps near the sheath edge and sharper plasma interfaces.

The results obtained, on the one hand, do not contradict the previous theoretical treatment of the potential distribution for complex plasma discharges predicting a potential jump of up to $\varphi \simeq 0.5T_e/e$ at the interface complex plasma/sheath for dense dust clouds due to the ionization of neutral atoms by 'hot' electrons [12, 13]. On the other hand, it seems that our findings are supported by measurements of the spatial distribution of microparticles in the monolayer crystals. What is needed now is more precise measurements of the particle coordinates within a 3D dust configuration in microgravity that would allow us to test this theoretical model more directly.

Finally, note that the problems of plasma boundaries and plasma–sheath interactions are quite generic, and the results presented here can also be relevant to other plasma systems involving highly charged tiny dust particles (e.g. in experiments on particle coagulation and agglomeration, for technological or processing plasmas).

Acknowledgments

MAH thanks the National Research Foundation for research grants. Any opinions, findings and conclusions or recommendations expressed in this material are those of the authors and therefore the NRF does not accept any liability in regard thereto.

References

[1] Havnes O *et al* 1984 *J. Geophys. Res.* **89** 10999
[2] Havnes O *et al* 1990 *J. Geophys. Res.* **95** 6581
[3] Luo H and Yu M Y 1997 *Phys. Rev.* E **56** 1270
[4] Goree J *et al* 1999 *Phys. Rev.* E **59** 007055
[5] Wang X and Bhattacharjee A 2000 *Phys. Plasmas* **7** 3093
[6] Annaratone B M *et al* 2002 *Phys. Rev.* E **66** 056411
[7] Bryant P M 2004 *New J. Phys.* **6** 60
[8] Tsytovich V N, Vladimirov S V and Benkada S 1999 *Phys. Plasmas* **6** 2972
[9] Tsytovich V N 2000 *Plasma Phys. Rep.* **26** 668
[10] Thomas E Jr 2001 *Phys. Plasmas* **8** 329
[11] Thomas E Jr *et al* 2002 *Phys. Rev.* E **66** 016405
[12] Yaroshenko V V, Thoma M H, Thomas H M and Morfill G E 2010 *IEEE Trans. Plasma Sci.* **38** 869
[13] Yaroshenko V V, Thoma M H, Thomas H M and Morfill G E 2008 *Phys. Plasmas* **15** 082104
[14] Yaroshenko V V, Verheest F, Thomas H M and Morfill G E 2009 *New J. Phys.* **11** 073013
[15] Nefedov A P *et al* 2003 *New J. Phys.* **5** 33
[16] Thomas H M *et al* 2008 *New J. Phys.* **10** 033036
[17] Piel A, Klindworth M, Arp O, Melzer A and Wolter M 2006 *Phys. Rev. Lett.* **97** 205009
[18] Piel A, Arp O, Klindworth M and Melzer A 2008 *Phys. Rev.* E **77** 026407
[19] Rothermel H, Hagl T, Morfill G E, Thoma M H and Thomas H M 2002 *Phys. Rev. Lett.* **89** 175001
[20] Mikikian M, Boufendi L, Bouchoule A, Thomas H M, Morfill G E, Nefedov A P, Fortov V E and the PKE-Nefedov team 2003 *New J. Phys.* **5** 19
[21] Ostrikov K, Denysenko I B, Vladimirov S V, Xu S, Sugai H and Yu M Y 2003 *Phys. Rev.* E **67** 056408

[22] Denysenko I B, Ostrikov K, Xu S, Sugai H, Yu M Y and Diong C H 2003 *J. Appl. Phys.* **94** 6097
[23] Gozadinos G, Ivlev A V and Boeuf J P 2003 *New J. Phys.* **5** 32
[24] Vaulina O S and Khrapak S A 2000 *J. Theor. Exp. Phys.* **90** 287
[25] Baboolal S, Bharuthram R and Hellberg M A 1990 *J. Plasma Phys.* **44** 1
[26] Verheest F and Hellberg M A 1997 *J. Plasma Phys.* **57** 465
[27] Nosenko V, Ivlev A V, Zhdanov S K, Fink M and Morfill G E 2009 *Phys. Plasmas* **16** 083708
[28] Hebner G A, Rilye M E and Greenberg K E 2002 *Phys. Rev.* E **66** 046407